

Adaptive Precoding for Femtocell Interference Mitigation

Ahmed R. Elsherif, Ahmed Ahmedin, Zhi Ding, and Xin Liu
University of California, Davis, California 95616
Email: {arelsherif,ahmedin,zding,xinliu}@ucdavis.edu

Abstract—In this paper¹, we study interference mitigation in cellular networks with femtocells. We propose to use adaptive distributed beamforming to mitigate downlink interference between femtocell users, known as Home User Equipments (HUEs), and macrocell users, known as Macrocell User Equipments (MUEs). We develop three MIMO beamforming schemes for interference mitigation that take into account the QoS requirement of femtocell and macrocell clients. These new heterogeneous MIMO precoding strategies improve flexibility in resource provisioning and signaling requirement in response to QoS need. The proposed schemes minimize the interference at the MUE or maximize the throughput at the HUE depending on the network traffic and QoS constraints. We also analyze the MUE mean throughput by applying order statistics theory.

I. INTRODUCTION

It has been shown that more than 50% of voice calls and more than 70% of data loads originate from indoor users [1]. However, current cellular networks provide poor indoor coverage, especially for data services because they often use high carrier frequencies that have large attenuation losses which degrades indoor coverage. Femtocells are considered a promising technology to address this issue. A femtocell is an indoor cellular base station that transmits to subscribers at a much reduced power using cellular spectrum. It uses a broadband connection such as Digital Subscriber Line (DSL), cable modem, or RF as a backhaul channel to communicate with the main cellular network.

From the network operator's point of view, femtocells improve indoor coverage, and offload traffic from the macrocell, which helps improve the macrocell throughput and link reliability. Moreover, the cost of femtocells, including equipment and deployment, is much less than that of a macrocell basestation deployed by the operator. The concept of femtocells has been already proposed in

the standardization process for next generation communication systems such as, LTE, LTE-A, and WiMAX [2]. Femtocells are referred to as Home eNB (HeNB) in LTE standardization.

The main challenge of femtocell-macrocell deployments is interference management due to transmission on the same frequency and at the same time by both femtocells and macrocells. Recent research work has attempted to address this problem. In [3], an adaptive power control technique is proposed to decrease the transmitting power of femtocells in order to maximize frame utilization. One major drawback of this scheme is that it is oblivious to the QoS need of macrocell user equipment (MUE) that experiences the HeNB interference.

In [4], the authors consider fixed probability assignment to physical resource blocks (PRBs), giving the home user equipment (HUE) higher access probability to the PRBs occupied by outdoor MUEs. However, this scheme requires signaling at the macro basestation (MBS). The work also needs more investigation in the case of multiple femtocells. In [5], an adaptive antenna technique that combines null steering and spectral band selection is proposed for cognitive radio networks. The same idea is applied on femtocells in [6].

Among existing works in the literature, there are two related publications [7] and [8] on beamforming techniques in multiple antenna systems for interference control. The scheme proposed in [7] addresses the interference problem between two HeNBs: HeNB₁ and HeNB₂. It assumes that the channel between HeNB₂ and its HUE is good enough so that HeNB₂ will choose the precoding matrix index that minimizes the mutual interference. This may not be always true because the channel between HeNB₂ and its HUE may suffer from distortions and losses such as multi-path fading.

The authors in [8] also consider the interference between MUE and HeNB, as in our paper here. The major difference is that the proposed solution in [8] requires a connection between MBS and HeNB which is done

¹This material is based upon works supported by the National Science Foundation under Grants 0917251 and 1147930

through the DSL backhaul. This leads to a significant delay which leads to performance degradation as the channel between MUE and HeNB varies rapidly. In our work, we overcome the delay issue by exploiting the MUE feedback signals decoded by the femtocells as part of the heterogeneous network. Moreover, the analysis in [8] rely on a strong assumption that the projection power of normalized channel vectors onto different beamforming directions generates a set of independent random variables. This assumption is not necessarily true, particularly for the codebooks defined in LTE standard releases for different antenna configurations.

The rest of the paper is organized as follows: The system model is presented in Section II. Three schemes are proposed in Section III. Mean throughput analysis of MUE is derived in Section IV. Numerical results are then presented in Section V for performance evaluation and verifications, followed by conclusion in Section VI.

II. SYSTEM MODEL

In this paper, we consider a heterogeneous network (HetNet) that consists of femtocells deployed in the coverage of a macrocell. The downlink mutual interference between HeNBs and MUEs is modeled as a Z-channel as shown in Fig. 1. The Z-channel model means that the transmission from the HeNB to the HUE causes interference to MUE, but the MBS transmission does not cause too much interference to the downlink reception at the HUE. This assumption is reasonable as the HeNB is mostly set up in places with weak coverage of the MBS. In this case, HeNB needs to adapt its transmission based on the channel gain between itself and the MUE, denoted as H_{10} , to reduce interference on the MUE. H_{00} and H_{11} are the direct channel gain vectors from the MBS to the MUE and from the HeNB to the HUE, respectively. All channel gains are assumed to be Rayleigh, i.e., complex Gaussian i.i.d. random variables.

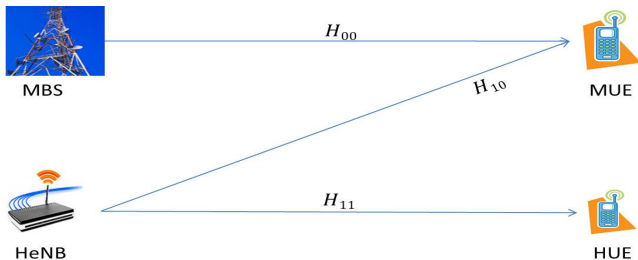


Fig. 1: Downlink interference channel model.

We assume that HeNB, HUE, and MUE are equipped with MIMO systems. A connection is established be-

tween the MUE and the interfering neighboring HeNB. The HeNB and the MUE are collaborating via feedback signals to perform beamforming. The beamforming index, namely the precoding matrix index (PMI), is chosen via certain criteria that will be explained later and then sent to the HUE to use it. The chosen PMI should be updated according to how fast the interference channel changes.

One may be concerned about the feasibility of setting up a connection between HeNB and MUE. In fact, this connection is practical and sometimes well-defined. In the LTE-A and UMTS standards, MUE may connect with more than one cell at the same time. The signaling overhead is insignificant as the femtocell typically serves very few users and, at the same time, the MUE only needs to transmit the indices of the chosen beamformers each time which consist of a few bits. For example, we need two bits in LTE-A for two transmit antennas and four bits for four transmit antennas. In addition, we do propose a scheme without this signaling connection in Section III for special applications.

During downlink beamforming, the received signal at the HUE is given by

$$\vec{r}_f = H_{11}\vec{w}_f s_f + n_f, \quad (1)$$

where s_f is the HeNB transmitted symbol, n_f is AWGN, and the vector w_f is the precoding matrix (beamforming weight) used by the HeNB. H_{11} denotes the MIMO channel matrix between HeNB and HUE with dimension $N_r^f \times N_t^f$ with N_r^f HUE receive antennas and N_t^f HeNB transmit antennas. In LTE-A, the beamforming vector $\vec{w}_f \in \mathcal{W}$, where \mathcal{W} is a finite set of all possible beamforming weights. Each vector $\vec{w}_f \in \mathcal{W}$ has a unit norm and a length of N_t^f . Similarly, the interference from the HeNB on the MUE is characterized by $H_{10}\vec{w}_f$. The following section discusses the possible criteria to choose the optimum \vec{w}_f among \mathcal{W} to satisfy the requirements of both MUE and HUE. We introduce the following notations to be used in the rest of the paper:

P_f : constant HeNB transmission power.

P_m : constant MBS transmission power.

\mathcal{W} : set of all precoders with cardinality K .

\mathcal{W}_m : set of MUE restricted precoders, with cardinality K_m , that satisfy the required criteria out of \mathcal{W} .

ϵ : interference power threshold that controls the MUE QoS, decreasing ϵ improves the MUE QoS.

η : interference power threshold that determines the HUE QoS, increasing η improves the MUE QoS.

III. PROPOSED SCHEMES

We propose three different schemes to choose the most suitable PMI based on the network requirements and priorities. The three schemes are based on using a restricted subset codebook which is supported in LTE [9]. The first scheme is ‘‘MUE Restricted Subset Codebook’’. This method gives priority to MUEs, and is, thus, suitable for heavily loaded macro networks and/or high priority macrocell traffic. The second scheme is ‘‘HUE Augmented PMI Feedback’’. This one targets the HUE QoS provisioning, which makes it more suitable for lightly loaded macro networks. The third is ‘‘HeNB Restricted Subset Codebook’’, which is a modification of the first one where HeNB can choose the PMI without the need of establishing connection with the MUE. The following subsections discuss the three schemes in detail.

A. MUE Restricted Subset (MRS) Codebook Precoding

In this scheme, a connection is established between the MUE and the interfering HeNB. This connection is used to exchange information between the HeNB and the MUE. First, MUE estimates the cross channel response H_{10} based on HeNB downlink reference signals (pilots). The MUE sends to the HeNB a subset of indices in the codebook that satisfies the following criterion

$$\mathcal{W}_m = \{\vec{w}_i : P_f \|H_{10}\vec{w}_i\|^2 \leq \epsilon\}. \quad (2)$$

Note that (2) characterizes the interference from the HeNB on the MUE and the choice of \mathcal{W}_m that satisfies the MUE interference constraint. The QoS concern expressed by the MUE as the maximum HeNB interference level is defined by ϵ . The smaller the value of ϵ , the higher the MUE priority. For real time traffic and in heavily loaded networks, ϵ can be very small to make the HeNB more conservative. After receiving the set of indices, \mathcal{W}_m , sent by the MUE, HeNB chooses the one that maximizes the SINR to its HUE as follows

$$\max_{\vec{w}_i \in \mathcal{W}_m} P_f \|H_{11}\vec{w}_i\|^2. \quad (3)$$

The flow of the algorithm and the required signaling are summarized in Fig. 2.

B. HUE Augmented PMI (HAPMI) Feedback

We now consider the scenario where we need to give higher priority to the HUE service quality. As in the MRS scheme, a connection is established between the HeNB and MUE. The index set that guarantees

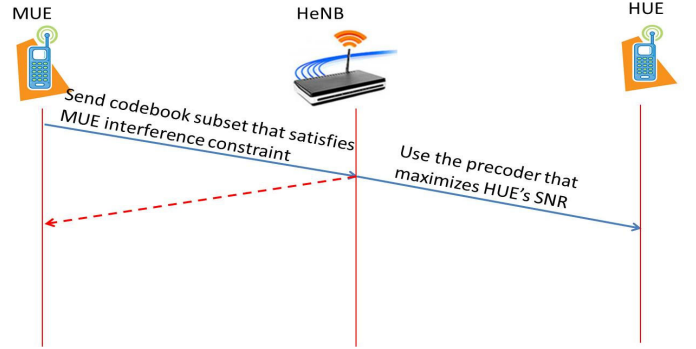


Fig. 2: MUE restricted subset codebook scheme.

acceptable performance for the HUE is sent to the MUE. This can be characterized as follows:

$$\mathcal{W}_f = \{\vec{w}_i : P_f \|H_{11}\vec{w}_i\|^2 \geq \eta\}. \quad (4)$$

The MUE receives the index set \mathcal{W}_f and estimates the cross channel with the HeNB using the pilot symbols in the same transmission that provided the index set \mathcal{W}_f . Based on the complex channel gain values, the MUE chooses the final beamformer \vec{w}_f that minimizes the cross channel interference via

$$\min_{\vec{w}_i \in \mathcal{W}_f} P_f \|H_{10}\vec{w}_i\|^2. \quad (5)$$

The MUE sends \vec{w}_i back to the HeNB to use. Fig. 3 summarizes this scheme.

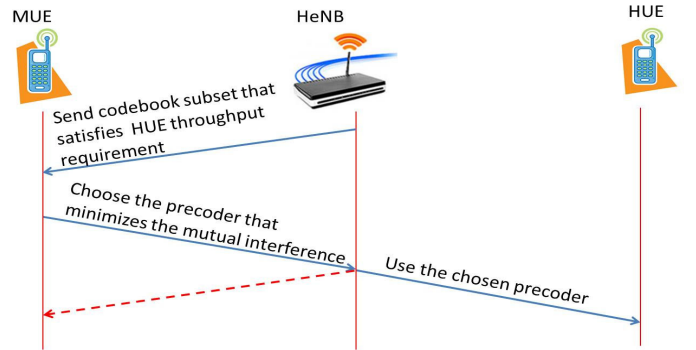


Fig. 3: HUE augmented PMI feedback scheme.

C. HeNB Restricted Subset (HRS) Codebook

This scheme can be considered as a modification of the MRS scheme where HeNB estimates the channel between itself and the MUE. This can be done by listening to the uplink feedback signals, and the reference signals therein, at the HeNB to get an estimate \tilde{H}_{10} of the actual downlink channel seen by the MUE, H_{10} . Based on channel reciprocity, we can apply (2) on the

reciprocally generated channel \tilde{H}_{10} between the MUE and the HeNB to determine a codebook subset \mathcal{W}_q , from which the PMI is obtained by applying (3) on the set \mathcal{W}_q .

The advantage here is that the decision is solely made at the HeNB and no signaling is needed between the MUE and the HeNB. However, performance may degrade if channel reciprocity does not hold. Thus, there is a trade-off between the signaling and the accuracy of the provided complex channel gain.

Table I compares the three proposed schemes in terms of the priority and the need for connection between MUE and the interfering HeNB.

Algorithm	Selection	Decision	Priority	Signaling
MRS	MUE	HeNB	MUE	Yes
HAPMI	HeNB	MUE	HUE	Yes
HRS	HeNB	HeNB	MUE	No

TABLE I: Comparison of the proposed algorithms.

IV. THROUGHPUT ANALYSIS

In this section, we analyze the mean throughput of the MUE for the MRS scheme. To analyze the mean throughput, we need to derive the probability density function (PDF) of the MUE's SINR. First, the SINR as seen by the MUE is given by

$$\text{SINR} = \frac{P_m \|H_{00}\|^2}{P_f \|H_{10} \vec{w}_{i^*}\|^2 + N_0}, \quad (6)$$

where \vec{w}_{i^*} is the precoding vector that satisfies both (2) and (3). We first define a real-valued random variable $u = \|H_{00}\|^2$ which has a chi-squared distribution with $2N_t^m$ degrees of freedom. We also define

$$x_i = \|H_{10} \vec{w}_i\|^2 \quad \forall i \in \{1 \dots K\}.$$

Given the previous definition of x_i , we further define v as a random variable chosen from the set \mathcal{W}_m that satisfies the condition in (2). In other words, if the values of $x_i \forall i \in \{1 \dots K\}$, are in an ascending order, then v is one of the first K_m ordered values. Given that each element of H_{10} is an i.i.d. complex Gaussian with zero mean and unit variance, and given that the beamformer vector is normalized to $\|w_i\|^2 = 1$, we can show that x_i is an exponential random variable with unit rate.

The PDF of v can be obtained using order statistics as in [12]. To simplify the analysis, we assume that $\{x_i\}$ are i.i.d. Strictly speaking, this i.i.d. assumption holds if and only if all codeword vectors are orthogonal, i.e., $\vec{w}_i^H \vec{w}_j = \delta[i - j]$. When the codebook contains vectors that are not always pairwise orthogonal, this

assumption is an approximation, and our analysis serves as an approximation to the true system throughput. Based on order statistics, the conditional PDF of v given the size of \mathcal{W}_m can be found as

$$f_v(v|K_m = L) = \sum_{\ell=1}^L Pr[\mathcal{M}_m(\ell) = i^*] g_{x_{(\ell)}}(v), \quad L > 0, \quad (7)$$

where $g_{x_{(\ell)}}(v)$ is the PDF of the ℓ -th smallest order statistic of $\{x\}$ and is given by

$$g_{x_{(\ell)}}(v) = a f_x(v) F_x(v)^{\ell-1} (1 - F_x(v))^{K-\ell}, \quad (8)$$

where $a = \frac{K!}{(K-\ell)!(\ell-1)!}$, $f_x(v)$ and $F_x(v)$ are the PDF and the cumulative distribution function (CDF) of the random variable $\{x\}$, respectively. Because x_i and y_i are independent, as H_{10} and H_{11} are independent, $Pr[\mathcal{M}_m(\ell) = i^*] = \frac{1}{L}$. Thus, the conditional PDF in (7) can be rewritten as

$$f_v(v|K_m = L) = \frac{1}{L} \sum_{\ell=1}^L g_{x_{(\ell)}}(v). \quad (9)$$

The PDF of v can be obtained by considering all possible values of the size of K_m as follows :

$$f_v(v) = \sum_{L=1}^K f_v(v|K_m = L) Pr[K_m = L]. \quad (10)$$

To find $Pr[K_m = L]$, we first define $p_i(\epsilon)$ as the probability that codeword \vec{w}_i satisfies the condition in (2). Thus, $p_i(\epsilon)$ can be written as

$$p_i(\epsilon) = Pr[x_i \leq \frac{\epsilon}{P_f}] = 1 - \exp(-\frac{\epsilon}{P_f}), \quad (11)$$

where we used the fact that x_i is a unit rate exponential random variable as proven earlier. Based on our earlier assumption that the random variables x_i are i.i.d, $p_i(\epsilon)$ will be the same for all codewords. Therefore, we drop the index i for simplicity and define $p(\epsilon) = p_i(\epsilon) \forall i \in \{1 \dots K_m\}$. Therefore, $Pr[K_m = L]$ becomes

$$Pr(K_m = L) = \binom{K}{L} (p(\epsilon))^L (1 - p(\epsilon))^{K-L} \quad (12)$$

Given PDFs of both u and v plus the fact that they are independent, the mean throughput can be determined as

$$\mathbb{E}(R) = B_m \int_u \int_v \log_2(1 + \text{SINR}) f_v(v) f_u(u) dv du. \quad (13)$$

Though the mean throughput analysis does not exhibit a closed form, it can be numerically evaluated via standard integration or importance sampling techniques [10], as shown in Section V.

V. SIMULATION RESULTS

In this section, we evaluate the performance of our proposed schemes. Two performance metrics are considered, namely, 5%-outage capacity and mean throughput. The 5%-outage capacity is given by C_0 , where

$$Pr(C(H) < C_0) = 0.05, \quad (14)$$

where $C(H)$ is the instantaneous capacity under a random channel realization H . On the other hand, the mean throughput is the ensemble average of instantaneous capacity over all channel realizations. The performance metrics are evaluated and shown against the distance between the MUE and the interfering HeNB. We compare the performance of the MRS, HAPMI, and HRS schemes described earlier with two other competing schemes representing performance bounds. The first one, labeled “*min interference*”, uses the PMI that minimizes the interference at the MUE, which does not consider the HUE throughput maximization (same as proposed in [7]). Hence, the performance of “*min interference*” constitutes an upper bound on the throughput of the MUE. The second scheme, labeled “*max throughput*”, uses the PMI that maximizes the throughput of the HUE while ignoring the interference seen by the MUE. This results in an upper bound on the throughput of the HUE.

For the case of two transmit antennas, we use 2 bits to encode the precoder matrix indexing (PMI) which is consistent with the LTE-A standard. The codebook for precoding is given in [11]. We also tested 4-bit indexing for which the simulation exhibited only marginal improvement. The simulation parameters are summarized in Table II. Channel gains are assumed to be complex Gaussian i.i.d. random variables.

Parameter	Value
Bandwidth(MUE/HUE)	1.08MHz
MUE/HUE Noise Figure	7dB
MBS Transmit Power	47dBm
HeNB Transmit Power	20dBm
MBS to MUE Path Loss	$151.1 + 42.8 \cdot \log_{10}(d_1/1000)$ d_1 : distance between HeNB & HUE
HeNB to HUE Path Loss	$127 + 30 \cdot \log_{10}(d_2/1000)$ d_2 : distance between MBS & MUE
HeNB # of Tx Antennas	2 or 4

TABLE II: Simulation Parameters.

Fig. 4 and 5 show the mean throughput and the 5%-outage capacity seen by both the MUE and the HUE, respectively, given two transmit antennas. As shown in Fig. 4 and 5, the system has the flexibility to give priority to MUE interference mitigation in heavily loaded networks

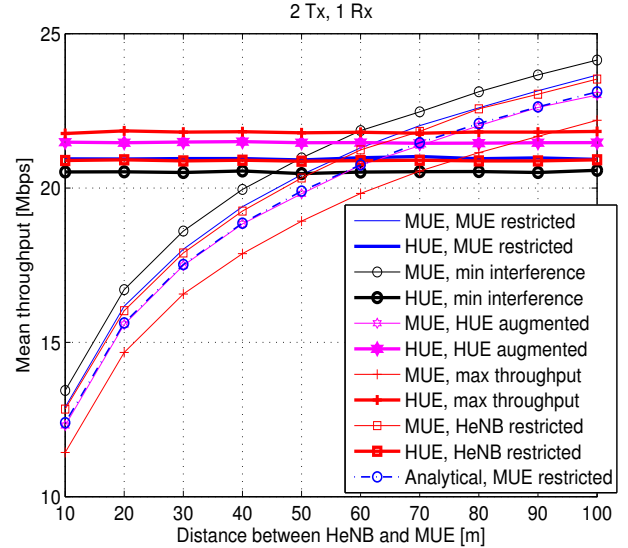


Fig. 4: Mean throughput for the proposed algorithms, 2 Tx antennas.

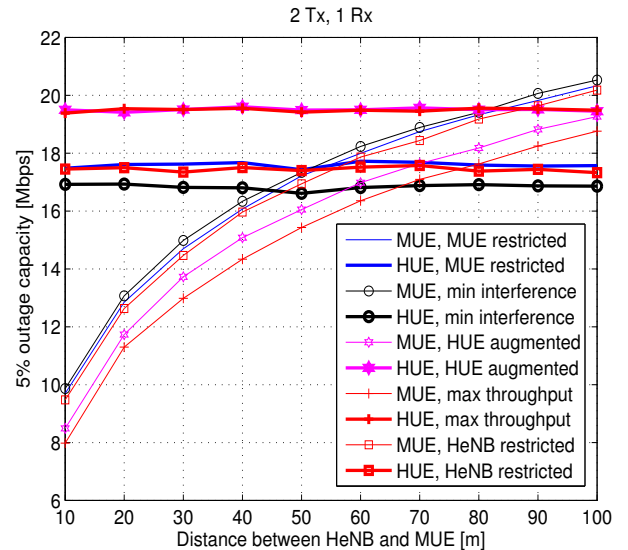


Fig. 5: 5%-outage capacity for the proposed algorithms, 2 Tx antennas.

or to HUE throughput maximization in lightly loaded networks. With respect to the MUE throughput, the “*min interference*” performance represents the upper bound whereas the “*max throughput*” performance represents the lower bound. On the other hand, the opposite is true with respect to the HUE performance. The threshold values ϵ and η can determine how the throughput of the MUE restricted or the HUE augmented scheme may edge toward one of the bounds depending on the user priorities.

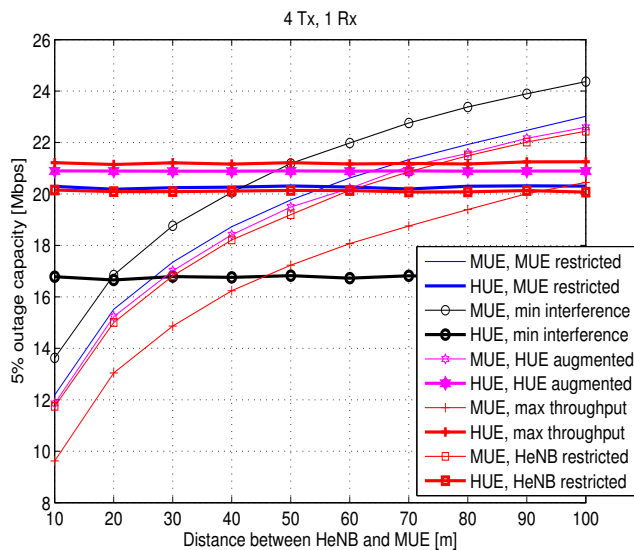


Fig. 6: 5%-outage capacity for the proposed algorithms, 4 Tx antennas.

For the HRS scheme, a reciprocity error is taken into account and modeled as a zero mean complex Gaussian random variable with a variance of 0.1. Fig. 4 and 5 show that the performance of the HRS scheme is very close to that of the MRS. Thus, the HRS scheme is capable of delivering comparable performance to the MRS scheme without the need for any connection between the HeNB and the MUE. In Fig. 4, we also provide numerical results using importance sampling on the mean throughput in (13) for the case of two antennas, marked as “Analytical, MUE restricted”. The gap seen between the analytical mean throughput in (13) and simulation results for the ensemble average of instantaneous capacity for different channel realizations is the direct consequence of non-orthogonal precoders in LTE-A standard.

Fig. 6 shows the 5%-outage capacity of both MUE and HUE in the case of four transmit antennas. We observe similar trends as in the case of two antennas but with a larger gap in performance among various schemes. This is expected as the codebook for four antennas has more codewords and, thus, the gain of properly selecting the best precoder becomes more obvious.

VI. CONCLUSION

In this work, we propose three practical schemes of interference control and mitigation in a heterogeneous LTE cellular network environment. The decision on which scheme to use depends on the QoS requirement of the MUE and the HUE as well as their QoS priorities. To avoid the need for a costly and impractical low delay

connection between HeNB and neighboring MUEs, one of our proposed schemes requires HeNB to estimate the channel between itself and the MUE by listening to feedback signals and pilots. The HeNB adapts the beamforming weight index based on the cross interference channel and the required QoS. Simulation results show that the system can adapt between MUE interference mitigation in dense networks and HUE throughput maximization in lightly loaded networks. In future works, we will investigate extensions to multiple MUEs and multiple HeNBs and develop precoding strategies for spatial multiplexing MIMO transmissions.

REFERENCES

- [1] Presentations by ABI Research, Picochip, Arivana, IP access, Gartner, Telefonica Espana, 2nd Int'l Conf. Home Access Points and Femtocells; http://www.avrenevents.com/dallas-femto2007/purchase_presentations.htm
- [2] J. Zhang and G. de la Roche, *Femtocells : Technologies and Deployment*, John Wiley & Sons, New York, NY, USA, 2010.
- [3] Pavel Mach, Zdenek Becvar, “Dynamic Power Control Mechanism for Femtocells Based on the Frame Utilization,” in *Wireless and Mobile Communications (ICWMC)*, 2010 6th International Conference.
- [4] Z. Zheng, J. Hmlinen, and Y. Yang, “On Uplink Power Control Optimization and Distributed Resource Allocation in Femtocell Networks,” in *VTC Spring 2011 BeFEMTO workshop*, 15 May, (Budapest, Hungary), 2011.
- [5] J. Mitola, “Cognitive radio for flexible mobile multimedia communications,” in *IEEE International Workshop on Mobile Multimedia Communications (MoMuC99)* (Cat. No.99EX384), vol. 22102, pp. 3-10, 1999.
- [6] M. Husso, J. Hamalainen, R. Jantti, and A. M. Wyglinski, “Adaptive Antennas and Dynamic Spectrum Management for Femtocellular Networks: A Case Study,” in *3rd IEEE Symposium on New Frontiers in Dynamic Spectrum Access Networks*, pp. 1-5, Oct. 2008.
- [7] M. Husso, Zhong Zheng, J. Hamalainen and E. Mutafungwa, “Dominant interferer mitigation in closed femtocell deployment,” in *IEEE 21st International Symposium on Personal Indoor and Mobile Radio Communications PIMRC 2010*. IEEE, 2010. 169-174.
- [8] J. Zhu and H. C. Yang, “Interference Control with Beamforming Coordination for Two-Tier Femtocell Networks and its Performance Analysis,” in *IEEE International Conference on Communications (ICC)*, 2011.
- [9] “Evolved Universal Terrestrial Radio Access (E-UTRA); Physical Layer Procedures (Release 10),” 3GPP TSG RAN TS 36.213, v10.3.0, Sep. 2011. [Online]. Available: <http://www.3gpp.org/ftp/Specs/archive/36%5Fseries/36.213/>
- [10] P. W. Glynn and D. L. Iglehart, “Importance sampling for stochastic simulations,” *Management Science*, vol. 35, no. 11, pp. 13671392, 1989.
- [11] “Evolved Universal Terrestrial Radio Access (E-UTRA); Physical Channels and Modulation (Release 10),” 3GPP TSG RAN TS 36.211, v10.3.0, Sep. 2011. [Online]. Available: <http://www.3gpp.org/ftp/Specs/archive/36%5Fseries/36.211/>
- [12] H. A. David, *Order Statistics*, vol. 54, no. 1. Wiley, 1981, pp. 2-7.